<Original Article>

# Comparison of teratogenecity induced by nano- and micro-sized particles of zinc oxide in cultured mouse embryos

**A Young Jung, Ki Youn Jung, Chunmei Lin, Jung-Min Yon, Jong Geol Lee, Beom Jun Lee,
Young Won Yun, Sang-Yoon Nam\***

*College of Veterinary Medicine and Research Institute of Veterinary Medicine, Chungbuk National University,
Cheongju 362-763, Korea*

**Abstract :** The increasing uses of zinc oxide nanoparticles (nZnO) in industrial and personal care products raise possible danger of using nZnO in human. To determine whether ZnO induces size-dependent anomalies during embryonic organogenesis, mouse embryos on embryonic day 8.5 were cultured for 2 days under 50, 100, and 150 µg of nZnO (< 100 nm) or micro-sized ZnO (mZnO; $80 \pm 25$ µm), after which the morphological changes, cumulative quantity of Zn particles, and expressions of antioxidant and apoptotic genes were investigated. Although embryos exposed to 50 µg of ZnO exhibited no defects on organogenesis, embryos exposed to over 100 µg of ZnO showed increasing anomalies. Embryos treated with 150 µg of nZnO revealed significant changes in Zn absorption level and morphological parameters including yolk sac diameter, head length, flexion, hindbrain, forebrain, branchial bars, maxillary process, mandibular process, forelimb, and total score compared to the same dose of mZnO-treated embryos. Furthermore, CuZn-superoxide dismutase, cytoplasmic glutathione peroxidase (GPx) and phospholipid hydroperoxidase GPx mRNA levels were significantly decreased, but caspase-3 mRNA level was greatly increased in nZnO-treated embryos as compared to normal control embryos. These findings indicate that nZnO has severer teratogenic effects than mZnO in developing embryos.

**Keywords :** micro-sized ZnO, nano-sized ZnO, teratogenesis, whole mount embryo culture, zinc oxide

## Introduction

Recently, a lot of nanomaterials have been produced and widely applied as a result of rapid development of nano-science, nanotechnology, and engineering [8, 11]. Nanoparticles (NPs) which are smaller than size of human cells (< 100 nm) have been extensively used in solar energy capture, cosmetics, electronics, and food and drug delivery systems and have also been utilized in biological applications that require long-term, multi-target, and highly sensitive imagings [4, 14, 22]. However, NPs have high catalytic activity and propensity to absorb, penetrate and be internalized within biological tissues and cells [16]. Therefore, possible harmful effects of NPs on human health and environmental safety have been increased [18, 26].

Zinc oxide NP (nZnO) is most commonly used and has attracted a special attention worldwide due to outstanding properties as compared to its bulk counterpart. The nZnO has been widely utilized in paint formulation, ceramic manufacture, photocatalysis, UV filters, biosensors, and personal care products such as toothpaste, sun cream, beauty care prod-

ucts, and hair care products [7, 11, 24]. However, toxicological and environmental effects of nZnO *via* its direct and indirect exposures are unclear yet.

The NPs are able to enter various kinds of membranes including the blood-brain barrier, the air-blood barrier in lung, and the gastro-intestinal wall, as well as the placenta and fetus of pregnant rat [23]. Previous studies have shown that nZnO has pulmonary toxicities in rat, guinea pig and rabbit [10], serious liver and kidney damages in mice [5], and toxicities in human bronchial epithelial cells and cardiac microvascular endothelial cells [12, 25]. nZnO down-regulated the expression of survivin along with activation of caspase-3 enzymes in human alveolar adenocarcinoma cells [1]. The cytotoxicities of nZnO are mediated through reactive oxygen species (ROS) generation and oxidative stress [13, 30]. George *et al.* [9] recently found that nZnO exposure could decrease the hatching rates of zebrafish embryo. Although embryogenesis is highly sensitive to oxidative damages such as ambient oxygen concentrations or the products of maternal disorders [3], it has not been clearly understood whether nZnO affects mammalian embryogenesis.

*Corresponding author
Tel: +82-43-261-2596,   Fax: +82-43-271-3246
E-mail: synam@cbu.ac.kr

In the present study, we examined the *in vitro* response of mouse embryo exposed to two types of ZnO particles (larger or smaller than 100 nm in size) in order to confirm the teratogenic effect of ZnO in cultured mouse embryo and determine the size- and dose-dependent toxicities of ZnO.

## Materials and Methods

### Chemicals and animals

Micro-sized ZnO ($80 \pm 25$ μm; mZnO) and nZnO ($< 100$ nm) powders (Sigma, USA) were diluted with saline. The suspensions were continuously dispersed for 1h by a bath sonicator to aid mixing and to maintain their stability. Male and female ICR mice (8~10 weeks old) were purchased from a commercial breeder (Biogenomics, Korea). One male and three female mice were housed in a cage for mating. The environmental conditions were controlled with an ambient temperature of $21 \pm 2$℃, relative humidity of $55 \pm 10\%$, air ventilation rate of 10 cycles per hour, and a 12:12 h light : dark cycle. The animals were fed standard mouse chow (Samyang, Korea) and tap water *ad libitum* throughout the experimental period. Pregnancy was confirmed the following morning (08:00) by the presence of vaginal plugs or spermatozoa detected in a vaginal smear collected after mating the previous evening (20:00). This was considered to be embryonic day (E) 0.5. Pregnant mice were sacrificed by cervical dislocation euthanasia on E 8.5, after which embryos were obtained. All experiments were approved and carried out according to the Guide for Care and Use of Animals (Chungbuk National University Animal Care Committee (CBNUA-588-13-02).

### Rat serum preparation

Serum of Sprague-Dawley male rats (10~12 weeks old) purchased from a commercial breeder (Biogenomics, Korea) was prepared as embryo culture fluid as follows. After collection, blood samples were immediately centrifuged for 10 min at $3,600 \times g$ and 4℃ to clear the plasma fraction of cells. The supernatant was then transferred to new tubes, which were centrifuged for 10 min at $3,600 \times g$ and 4℃ to separate the blood cells. The clear serum supernatant was subsequently decanted and pooled, after which the pooled serum was heat-inactivated for 30 min at 56℃ in a water bath. The samples were then used immediately or stored at −70℃. Serum was incubated at 37℃ and passed through a 0.2 μm filter prior to use in the whole embryo culture.

### Whole embryo culture and ZnO treatments

The whole embryo culture system was based on a previously described model [19]. Briefly, animals were sacrificed by cervical dislocation at E8.5 between 09:00 and 10:00, and only embryos with somite number of 4~8 were utilized. After removal of the decidua and Reichert's membranes, embryos with intact visceral yolk sacs and ectoplacental cones were randomly placed into sealed culture bottles (three embryos/bottle) containing 3 mL of culture medium and different con-

centrations (50, 100, and 150 μg/mL) of nZnO or mZnO dissolved in saline. In preliminary studies, the embryos exposed to both nZnO and mZnO at lower concentration than 50 μg/mL did not appear any defects on the growth and development during organogenesis in mice (data not shown). Therefore, ZnO quantities to check the embryonic toxicity were determined at the concentrations of 50, 100, and 150 μg/mL in culture serum. The culture bottles were initially gassed with a mixture of 5% $O_2$, 5% $CO_2$, and 90% $N_2$ over a 17 h period at a flow rate of 150 mL/min. Subsequent gassing was performed at the same rate over 7 h (20% $O_2$, 5% $CO_2$, and 75% $N_2$) and 24 h (40% $O_2$, 5% $CO_2$, and 55% $N_2$). All embryos were cultured for 48 h using a whole embryo culture system (Ikemoto Rika Kogyo, Japan).

### Morphological scoring

At the end of the 48 h culture period, embryos were evaluated according to a morphological scoring system developed by Van Maele-Fabry *et al.* [27]. Only viable embryos with yolk sac circulation and a heartbeat were utilized for morphological scoring. Measurements of each viable embryo were obtained with 17 standard scoring items for development, plus the yolk sac diameter, crown-rump length, and head length for growth. The developmental features that were assessed included the embryonic flexion, heart, neural tube, brain (forebrain, midbrain, and hindbrain), otic and optic systems, olfactory organs, branchial bars, maxilla, mandible, limb buds (forelimb and hindlimb buds), yolk sac circulation, allantois, and somites.

### Zn content analysis

Embryos were taken out and washed with phosphate buffered saline. Embryos were weighed, digested and analyzed for Zn content. Briefly, prior to elemental analysis, the embryos were digested in 70% nitric acid. After adding hydrogen peroxide, the mixture was heated at about 160℃ using a high-pressure reaction container in an oven chamber until the samples were completely digested. The solutions were then heated to remove the remaining nitric acid until the solutions were colorless and clear. Finally, the remaining solution was diluted to 5 mL with autoclaved water. Inductively coupled plasma mass spectrometry (ICP-MS; Varian 820-MS; Palo Alto, USA) was used to analyze the Zn concentration in the embryos.

### Quantitative real-time PCR analysis

Total RNA was isolated from cultured mouse embryos using a TRIzol Reagent (Invitrogen, USA) according to the manufacturer's protocol. Total RNA concentrations were determined by UV absorbance, after which total RNA (2 μg) was used in a cDNA Synthesis kit (Invitrogen). Real-time PCR was carried out in a 20 μg reaction volume using a SYBR Green Master Mix (Applied Biosystems, USA) and mouse embryonic cDNA (1.6 μg) as the template. Reactions were performed using a 7500 Real-Time PCR System (Applied

**Table 1.** Primer sequences used in the study

| Gene | Sequence (5' - 3') | Accession number |
|---|---|---|
| β-actin | forward : TTT CCA GCC TTC CTT CTT GGG TAT G<br>reverse : CAC TGT GTT GGC ATA GAG GTC TTA C | NM_007393 |
| CuZn-SOD | forward : TGC GTG CTG AAG GGC GAC<br>reverse : GTC CTG ACA ACA CAA CCT GGT TC | NM_011434 |
| cGPx | forward : TGT TTG AGA AGT GCG AAG TG<br>reverse : GTG TTG GCA AGG CAT TCC | NM_008160 |
| PHGPx | forward : TAA GAA CGG CTG CGT GGT<br>reverse : GTA GGG GCA CAC ACT TGT AGG | NM_008162 |
| Caspase-3 | forward : AAA GCC GAA ACT CTT CA TCA T<br>reverse : GTC CCA CTG TCT GTC TCA | NM_009810 |

Biosystems), according to the manufacturer's instructions. Gene-specific primers were designed by TIB Mol-Bio Synthesis (Germany). Primers to mouse cytoplasmic superoxide dismutase (CuZn-SOD), cytoplasmic glutathione peroxidase (cGPx), phospholipid hydroperoxide GPx (PHGPx), and caspase-3 were used. In addition, beta-actin primers were used as an internal standard to normalize target transcript expression (Table 1). Data were analyzed from nine independent runs using a comparative Ct method, as previously described by Livak and Schmittgen [17].

### Statistical analysis

Group differences were assessed *via* one-way analysis of variance (ANOVA) followed by Tukey's multiple comparison test. All analyses were conducted using the SPSS for Windows software (ver. 10.0; SPSS, USA). Morphological score data were compared using Kruskal-Wallis non-parametric ANOVA and Dunn's multiple comparison *post hoc* test. A $p < 0.05$ was considered significant. All data are expressed as the mean ± SE.

## Results

### Organogenic changes in embryos exposed to ZnO

The embryos exposed to 50 μg of both mZnO and nZnO had no defects in the growth and development of embryos with surrounding yolk sacs (Fig. 1B1 and C1; Fig. 2B1 and C1; Table 2). However, embryos exposed to 100 μg of mZnO or nZnO showed slightly decreased sizes, thinned yolk sac walls, and abnormal yolk sac circulations (Fig. 1B2 and C2; Fig. 2B2 and C2) and exhibited anomalies in the growth and development of mainly yolk sac diameter, heart, hindbrain, midbrain, forebrain, otic system, optic system, maxillary process, mandibular process, and olfactory system. All these abnormalities were severer in nZnO-treated embryos than mZnO-treated embryos (Table 2). Embryos exposed to 150 μg of both ZnO particles showed more severe abnormal yolk sac and embryonic features (Fig. 1B3 and C3; Fig. 2B3 and C3). The morphological scores were significantly decreased compared to those of control embryos (Table 2). Yolk sacs
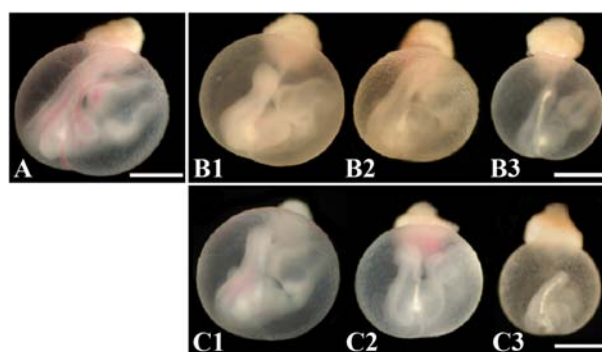


**Fig. 1.** Yolk sac developments in embryos cultured with nano- or micro-sized zinc oxide (nZnO or mZnO) for 48 h. Control embryo (A) showed normal yolk sac vessel and size development with typical vitelline vein and artery. Embryos treated with 50 μg (B1 and C1), 100 μg (B2 and C2), and 150 μg (B3 and C3) of mZnO or nZnO, respectively. ZnO treatments showed abnormal yolk sac vascularizations and remarkably smaller sizes than those of control embryos. These changes were more severe in nZnO-treated embryos than mZnO-treated embryos. Scale bar = 1 mm.
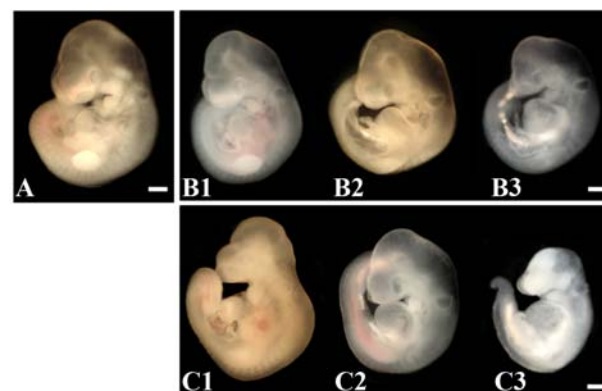


**Fig. 2.** Morphological changes in embryos cultured with nano- or micro-sized zinc oxide (nZnO or mZnO) for 48 h. Control embryo (A) showed normal embryonic feature. Embryos treated with 50 μg (B1 and C1), 100 μg (B2 and C2), and 150 μg (B3 and C3) of mZnO or nZnO, respectively. Morphological anomalies were more severe in nZnO-treated embryos than mZnO-treated embryos. Scale bar = 500 μm.

**Table 2.** Organogenic changes in the embryos exposed to nano- or micro-sized zinc oxide (nZnO or mZnO)

| Items | Dose of ZnO | | | | | | |
|---|---|---|---|---|---|---|---|
| | 0 | 50 µg | | 100 µg | | 150 µg | |
| | Control | mZnO | nZnO | mZnO | nZnO | mZnO | nZnO |
| | n = 32 | n = 22 | n = 23 | n = 27 | n = 30 | n = 30 | n = 30 |
| Yolk sac diameter (mm) | $3.37 \pm 0.06$ | $3.14 \pm 0.06$ | $3.07 \pm 0.09$ | $2.88 \pm 0.07^a$ | $2.62 \pm 0.06^{a,b,c}$ | $2.66 \pm 0.06^{a,b,c}$ | $2.27 \pm 0.04^{a,b,c,d,e,f}$ |
| Crown-rump length (mm) | $2.81 \pm 0.04$ | $2.74 \pm 0.04$ | $2.68 \pm 0.06$ | $2.61 \pm 0.06$ | $2.39 \pm 0.05^{a,b,c}$ | $2.31 \pm 0.06^{a,b,c}$ | $1.96 \pm 0.07^{a,b,c,d,e}$ |
| Head length (mm) | $1.30 \pm 0.02$ | $1.32 \pm 0.02$ | $1.32 \pm 0.03$ | $1.28 \pm 0.03$ | $1.16 \pm 0.04^b$ | $1.12 \pm 0.03^{a,b,c}$ | $0.88 \pm 0.04^{a,b,c,e,f}$ |
| Yolk sac circulation | $4.05 \pm 0.06$ | $4.02 \pm 0.06$ | $4.02 \pm 0.04$ | $3.89 \pm 0.07$ | $3.62 \pm 0.06^{a,b,c,d}$ | $3.59 \pm 0.05^{a,b,c,d}$ | $3.37 \pm 0.05^{a,b,c,d}$ |
| Allantois | $2.06 \pm 0.04$ | $2.02 \pm 0.03$ | $1.91 \pm 0.05$ | $1.94 \pm 0.04$ | $1.76 \pm 0.07^{a,b,d}$ | $1.70 \pm 0.05^{a,b,d}$ | $1.43 \pm 0.05^{a,b,c,d}$ |
| Flexion | $4.95 \pm 0.03$ | $4.95 \pm 0.02$ | $4.62 \pm 0.13$ | $4.78 \pm 0.08$ | $4.36 \pm 0.11^{a,b}$ | $4.49 \pm 0.12^a$ | $3.76 \pm 0.18^{a,b,c,d,f}$ |
| Heart | $4.78 \pm 0.05$ | $4.65 \pm 0.10$ | $4.51 \pm 0.12$ | $4.42 \pm 0.09^a$ | $3.98 \pm 0.08^{a,b,c}$ | $3.98 \pm 0.09^{a,b,c}$ | $3.54 \pm 0.10^{a,b,c,d}$ |
| Hindbrain | $4.44 \pm 0.12$ | $4.63 \pm 0.08$ | $4.27 \pm 0.11$ | $4.02 \pm 0.06^{a,b}$ | $3.80 \pm 0.09^{a,b,c}$ | $3.91 \pm 0.07^{a,b}$ | $3.46 \pm 0.08^{a,b,c,d,f}$ |
| Midbrain | $4.68 \pm 0.07$ | $4.83 \pm 0.08$ | $4.48 \pm 0.11$ | $4.07 \pm 0.07^{a,b}$ | $3.79 \pm 0.08^{a,b,c}$ | $3.83 \pm 0.08^{a,b,c}$ | $3.41 \pm 0.08^{a,b,c,d}$ |
| Forebrain | $5.53 \pm 0.10$ | $5.45 \pm 0.14$ | $5.08 \pm 0.20$ | $4.14 \pm 0.10^{a,b,c}$ | $3.94 \pm 0.11^{a,b,c}$ | $3.93 \pm 0.09^{a,b,c}$ | $3.38 \pm 0.09^{a,b,c,d,e,f}$ |
| Otic system | $4.92 \pm 0.03$ | $4.83 \pm 0.06$ | $4.66 \pm 0.11$ | $4.31 \pm 0.09^{a,b}$ | $4.13 \pm 0.08^{a,b,c}$ | $4.29 \pm 0.10^a$ | $3.78 \pm 0.12^{a,b,c}$ |
| Optic system | $4.95 \pm 0.02$ | $4.83 \pm 0.06$ | $4.64 \pm 0.11$ | $4.30 \pm 0.09^{a,b}$ | $4.13 \pm 0.09^{a,b,c}$ | $4.14 \pm 0.08^{a,b,c}$ | $3.60 \pm 0.11^{a,b,c,d}$ |
| Branchial bars | $3.44 \pm 0.07$ | $3.57 \pm 0.11$ | $3.43 \pm 0.12$ | $3.19 \pm 0.09$ | $2.70 \pm 0.07^{a,b,c,d}$ | $2.79 \pm 0.13^{a,b,c}$ | $2.07 \pm 0.13^{a,b,c,d,f}$ |
| Maxillary process | $2.90 \pm 0.03$ | $2.73 \pm 0.08$ | $2.61 \pm 0.10$ | $2.20 \pm 0.11^{a,b}$ | $1.77 \pm 0.07^{a,b,c}$ | $1.86 \pm 0.06^{a,b,c}$ | $1.39 \pm 0.05^{a,b,c,d,f}$ |
| Mandibular process | $2.83 \pm 0.09$ | $2.60 \pm 0.09$ | $2.51 \pm 0.10$ | $2.15 \pm 0.10^{a,b}$ | $1.72 \pm 0.06^{a,b,c}$ | $1.74 \pm 0.06^{a,b,c}$ | $1.25 \pm 0.05^{a,b,c,d,e,f}$ |
| Olfactory system | $2.78 \pm 0.06$ | $2.50 \pm 0.14$ | $2.35 \pm 0.15$ | $1.79 \pm 0.15^{a,b}$ | $1.03 \pm 0.10^{a,b,c,d}$ | $0.75 \pm 0.10^{a,b,c,d}$ | $0.49 \pm 0.07^{a,b,c,d}$ |
| Caudal neural tube | $5.00 \pm 0.00$ | $5.00 \pm 0.00$ | $4.90 \pm 0.06$ | $4.98 \pm 0.01$ | $4.84 \pm 0.07$ | $4.65 \pm 0.10$ | $4.20 \pm 0.14^{a,b,c,d,e}$ |
| Forelimb | $2.88 \pm 0.05$ | $2.72 \pm 0.08$ | $2.72 \pm 0.08$ | $2.59 \pm 0.07$ | $2.37 \pm 0.09^a$ | $2.38 \pm 0.13^a$ | $1.63 \pm 0.10^{a,b,c,d,e,f}$ |
| Hindlimb | $0.77 \pm 0.12$ | $0.44 \pm 0.11$ | $0.54 \pm 0.14$ | $0.42 \pm 0.11$ | $0.22 \pm 0.07^a$ | $0.09 \pm 0.03^a$ | $0.03 \pm 0.03^{a,b,c}$ |
| Somites | $4.03 \pm 0.03$ | $3.95 \pm 0.04$ | $4.04 \pm 0.04$ | $4.00 \pm 0.00$ | $3.93 \pm 0.04$ | $3.93 \pm 0.04$ | $3.53 \pm 0.09^{a,c,d}$ |
| Total score | $64.65 \pm 0.61$ | $63.76 \pm 0.92$ | $57.00 \pm 1.43$ | $61.30 \pm 1.07^{a,b}$ | $52.06 \pm 0.95^{a,b,c}$ | $52.07 \pm 1.12^{a,b,c}$ | $44.33 \pm 1.22^{a,b,c,d,e,f}$ |

Data are presented as the mean ± SE. [a]Control vs. ZnO groups ($p < 0.05$). [b]mZnO (50 µg) vs. nZnO (50, 100, and 150 µg) or mZnO (100 and 150 µg) groups ($p < 0.05$). [c]nZnO (50 µg) vs. mZnO (100 and 150 µg) or nZnO (100 and 150 µg) groups ($p < 0.05$). [d]mZnO (100 µg) vs. nZnO (100 and 150 µg) or mZnO (150 µg) groups ($p < 0.05$). [e]nZnO (100 µg) vs. mZnO (150 µg) or nZnO (150 µg) groups ($p < 0.05$). [f]mZnO (150 µg) vs. nZnO (150 µg) group ($p < 0.05$).

and embryos exposed to 150 µg of both mZnO and nZnO appeared opaque with few or no blood islands (Fig. 1B3 and C3; Fig. 2B3 and C3). Furthermore, morphological parameters such as yolk sac diameter, crown-rump length, head length, yolk sac circulation, allantois, heart, hindbrain, midbrain, forebrain, optic system, branchial bars, maxillary process, mandibular process, and olfactory system significantly decreased by the treatments with 150 µg of both mZnO and nZnO as compared to those of the low concentration groups. Specifically, 150 µg of nZnO diminished significantly the morphological parameters including yolk sac diameter, head length, flexion, hindbrain, forebrain, branchial bars, maxillary process, mandibular process, forelimb, and total score in the embryos as compared to the same dose of mZnO-treated embryos (Table 2). Morphological scores in the embryos exposed to ZnO were significantly decreased in concentration- and size-dependent manners ($p < 0.05$).
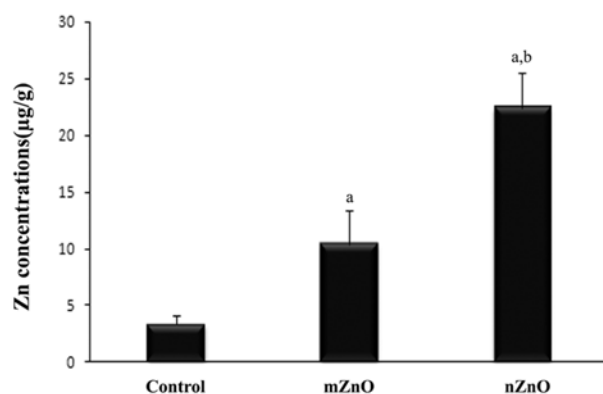


**Fig. 3.** Soluble Zn levels in embryos exposed to 150 µg of nano- or micro-sized zinc oxide (nZnO or mZnO) using inductively coupled plasma mass spectrometry analysis. Each value (n = 20) represents the mean ± SE. a; vs. control group, b; vs. mZnO group at $p < 0.05$.
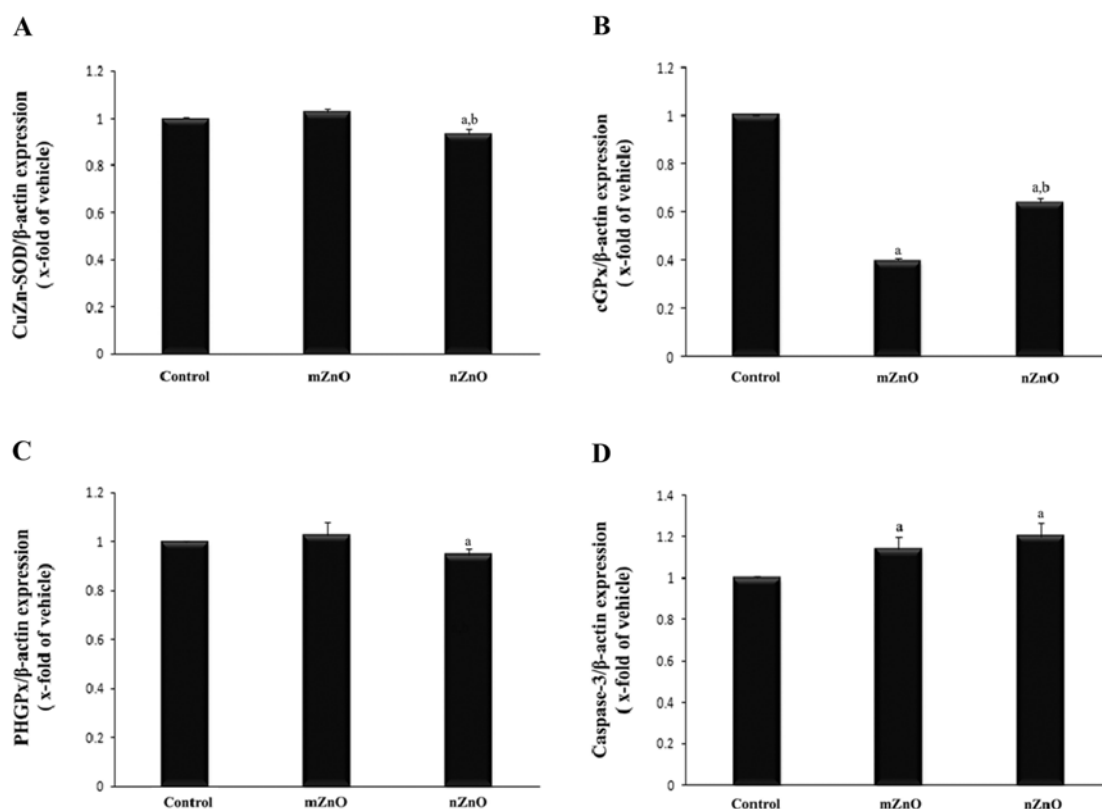
**Fig. 4.** Quantitative real-time PCR analyses of cytoplasmic superoxide dismutase (CuZn-SOD; A), cytoplasmic glutathione peroxidase (cGPx; B), phospholipid hydroperoxidase GPx (PHGPx; C), and caspase-3 (D) mRNAs in the mouse embryos exposed to 150 μg of nano- or micro-sized zinc oxide (nZnO or mZnO) for 2 days *in vitro*. Each value (n = 10) represents the mean ± SE. a; *vs.* control group, b; *vs.* mZnO group at $p < 0.05$.

### Zn cumulative levels in ZnO-treated embryos

In order to confirm Zn levels in embryos exposed to ZnO, Zn concentration was analyzed in embryos with surrounding yolk sac by ICP-MS assay. Zn contents were significantly increased in embryos exposed to 150 μg of both mZnO and nZnO as compared to those of the control embryos. Moreover, Zn content level was higher in nZnO-treated embryos than mZnO-treated embryos (Fig. 3; $p < 0.05$).

### Expression patterns of antioxidant enzyme genes in ZnO-treated embryos

As compared to the control embryos, CuZn-SOD mRNA level was significantly decreased in embryos exposed to 150 μg of nZnO, but was not different in embryos exposed to 150 μg of mZnO (Fig. 4A; $p < 0.05$). cGPx mRNA expression were significantly decreased in embryos exposed to 150 μg of both mZnO and nZnO compared to the control embryos ($p < 0.05$). Each cGPx mRNA level was 0.39- and 0.64-fold of control group (1-fold), respectively (Fig. 4B; $p < 0.05$). PHGPx mRNA level was significantly decreased in embryos exposed to 150 μg of nZnO compared to control embryos ($p < 0.05$). However, PHGPx mRNA level in embryos exposed to 150 μg of mZnO was not different from the control embryos (Fig. 4C).

### Expression patterns of caspase-3 mRNA in ZnO-treated embryos

Caspase-3 mRNA was significantly increased in embryos exposed to 150 μg of both mZnO and nZnO to 1.14- and 1.2-fold, respectively as compared to control embryos ($p < 0.05$). However, there was no difference between mZnO and nZnO embryos (Fig. 4D).

## Discussion

Due to the versatile use of NPs in consumer products, the possibility of their entrance into mammals and environment is increasing [29]. Therefore, it is necessary to investigate typical toxicological effects of NPs *via* a direct exposure into mammalian ecosystems.

During pregnancy, maternal and fetal metabolic disturbances caused by nZnO exposure have potentially detrimental effects on embryo development [32, 35]. ZnO-treated embryos remain unhatched and reveal bent spines in zebrafish [9] and the mice treated with nano-zinc suspensions show the symptoms such as lethargy, nausea, vomiting, abdominal cramps and diarrhea [28]. In the present study, the toxic effects in cases of different sizes and doses of ZnO on mouse embry-

onic organogenesis were evaluated. Embryos exposed to 50 µg of mZnO and nZnO had no defects on the growth and development of both yolk sac and embryos. However, embryos exposed to 100 µg of mZnO and nZnO showed slightly abnormalities and further severe anomalies were observed in the embryos treated with 150 µg of mZnO and nZnO. In particular, nZnO embryos showed more toxic effects than mZnO embryos. These findings indicate that ZnO is toxic to embryos at doses of over 100 µg and further nZnO is more detrimental to the embryo than mZnO.

The uptake and translocation of nano-ZnO into zebrafish inhibit embryo development [33]. NPs of ZnO are accumulated within cells and penetrate into organism easily with their size decreasing, leading to an oxidative stress response to the cells [33]. In the present study, Zn absorption into embryo was increased when the particle size of ZnO was decreased and morphological defects by ZnO exposure were the most remarkable in the nZnO-treated embryos, indicating that nZnO could permeate easily into yolk sac and embryo than mZnO and subsequently affect the development of each organ. Therefore, the absorption of ZnO into embryo could be elevated with its size decreasing and embryo toxicity might be caused by accumulation of ZnO during organogenesis. This result is also consistent with previous experimental data under fine and nano-particle exposure conditions *in vivo* [23].

An oxidative damage by single-wall carbon nanotubes is a main pathogenic mechanism in malformed placentas and embryos [21]. Embryogenesis seems to be very sensitive to high levels of ROS during early organogenesis [20]. Cellular oxidative stress and ROS generation have been understood as a possible mechanism of NPs' toxicity [1]. ROS affect the developing embryo by increase of oxidative stress and weak antioxidant defense [20]. In the present study, mRNA levels of the representative antioxidant enzymes such as CuZn-SOD, cGPx and PHGPx were significantly decreased in nZnO-exposed embryos than mZnO-exposed embryos. CuZn-SOD is an antioxidant enzyme that converts superoxide to hydrogen peroxide in cells and is detected in embryos and extraembryonic tissues from E8.5 to 18.5 of mouse [31]. cGPx mRNA is also an ubiquitous antioxidant that is expressed in developing mouse embryos on E7.5-18.5 cell- and tissue-specifically [2]. Furthermore, PHGPx is a unique antioxidant enzyme to reduce peroxidized phospholipids within biomembranes that is detected in fetal tissues such as telencephalon, diencephalon, spinal cord, and spinal ganglion on E13.5-18.5 of mouse [15]. These findings suggest that embryos are highly susceptible to the exposure to ZnO NPs and oxidative stress might be the primary mechanism for nZnO toxicity in mouse embryos.

Apoptosis induces programmed cell death in reply to various intrinsic or extrinsic death signals and is proved by series of cysteine proteases known as caspases [6, 34]. ZnO nanorod induces apoptosis in human alveolar adenocarcinoma cells [1]. Furthermore, pro-apoptotic caspase-3 acts as an excel-

lent molecular biomarker to assess the apoptotic response of NPs [34]. In the present study, caspase-3 mRNA expression was higher in nZnO-treated embryos than normal control and mZnO-treated embryos. These results suggest that upregulation of caspase-3 might be involved in the toxic effect of nZnO on mouse embryonic organogenesis.

In conclusion, nZnO promoted anomalies in mouse embryos by disturbances of antioxidant and cell survival systems in size- and dose-dependent manners as compared to mZnO, suggesting that nZnO has more severe teratogenic effects than mZnO in developing embryos.

## Acknowledgments

## References

1. **Ahamed M, Akhtar MJ, Raja M, Ahmad I, Siddiqui MKJ, AlSalhi MS, Alrokayan SA.** ZnO nanorod-induced apoptosis in human alveolar adenocarcinoma cells via p53, survivin and bax/bcl-2 pathways: role of oxidative stress. Nanomedicine 2011, **7**, 904-913.
2. **Baek IJ, Yon JM, Lee BJ, Yun YW, Yu WJ, Hong JT, Ahn B, Kim YB, Kim DJ, Kang JK, Nam SY.** Expression pattern of cytosolic glutathione peroxidase (cGPx) mRNA during mouse embryogenesis. Anat Embryol (Berl) 2005, **209**, 315-321.
3. **Burton GJ, Hempstock J, Jauniaux E.** Oxygen, early embryonic metabolism and free radical-mediated embryopathies. Reprod Biomed Online 2003, **6**, 84-96
4. **Chen D.** Design, synthesis and properties of highly functional nanostructured photocatalysts. Recent Pat Nanotechnol 2008, **2**, 183-189.
5. **Esmaeillou M, Moharamnejad M, Hsankhani R, Tehrani AA, Maadi H.** Toxicity of ZnO nanoparticles in healthy adult mice. Environ Toxicol Pharmacol 2013, **35**, 67-71.
6. **Fadeel B, Orrenius S.** Apoptosis: basic biological phenomenon with wide-ranging implications in human disease. J Intern Med 2005, **258**, 479-517.
7. **Fan Z, Lu JG.** Zinc oxide nanostructures: synthesis and properties. J Nanosci Nanotechnol 2005, **5**, 1561-1573.
8. **Farré M, Gajda-Schrantz K, Kantiani L, Barceló D.** Ecotoxicity and analysis of nanomaterials in the aquatic environment. Anal Bioanal Chem 2009, **393**, 81-95.
9. **George S, Xia T, Rallo R, Zhao Y, Ji Z, Lin S, Wang X, Zhang H, France B, Schoenfeld D, Damoiseaux R, Liu R, Lin S, Bradley KA, Cohen Y, Nel AE.** Use of a high-throughput screening approach coupled with in vivo zebrafish embryo screening to develop hazard ranking for engineered nanomaterials. ACS Nano 2011, **5**, 1805-1817.
10. **Gordon T, Chen LC, Fine JM, Schlesinger RB, Su WY,**

Kimmel TA, Amdur MO. Pulmonary effects of inhaled zinc oxide in human subjects, guinea pigs, rats, and rabbits. Am Ind Hyg Assoc J 1992, **53**, 503-509.

11. **Handy RD, von der Kammer F, Lead JR, Hassellöv M, Owen R, Crane M.** The ecotoxicology and chemistry of manufactured nanoparticles. Ecotoxicology 2008, **17**, 287-314.

12. **Heng BC, Zhao X, Xiong S, Ng KW, Boey FY, Loo JS.** Toxicity of zinc oxide (ZnO) nanoparticles on human bronchial epithelial cells (BEAS-2B) is accentuated by oxidative stress. Food Chem Toxicol 2010, **48**, 1762-1766.

13. **Huang CC, Aronstam RS, Chen DR, Huang YW.** Oxidative stress, calcium homeostasis, and altered gene expression in human lung epithelial cells exposed to ZnO nanoparticles. Toxicol In Vitro 2010, **24**, 45-55.

14. **Jaiswal JK, Simon SM.** Potentials and pitfalls of fluorescent quantum dots for biological imaging. Trends Cell Biol 2004. **14**, 497-504.

15. **Jung KY, Yon JM, No KO, Baek IJ, Lin C, Jun AY, Lee JG, Lee BJ, Yun YW, Nam SY.** Expression pattern of phospholipid hydroperoxide glutathione peroxidase mRNA during mouse fetal organ development. J Biomed Res 2010, **11**, 235-242.

16. **Klaine SJ, Alvarez PJJ, Batley GE, Fernandes TF, Handy RD, Lyon DY, Mahendra S, McLaughlin MJ, Lead JR.** Nanomaterials in the environment: behavior, fate, bioavailability, and effects. Environ Toxicol Chem 2008, **27**, 1825-1851.

17. **Livak KJ, Schmittgen TD.** Analysis of relative gene expression data using real-time quantitative PCR and the $2^{-\Delta\Delta C_T}$ method. Methods 2001, **25**, 402-408.

18. **Nel A, Xia T, Mädler L, Li N.** Toxic potential of materials at nanolevel. Science 2006, **311**, 622-627.

19. **New DA.** Whole-embryo culture and the study of mammalian embryos during organogenesis. Biol Rev Camb Philos Soc 1978, **53**, 81-122.

20. **Ornoy A.** Embryonic oxidative stress as a mechanism of teratogenesis with special emphasis on diabetic embryopathy. Reprod Toxicol 2007, **24**, 31-41.

21. **Pietroiusti A, Massimiani M, Fenoglio I, Colonna M, Valentini F, Palleschi G, Camaioni A, Magrini A, Siracusa G, Bergamaschi A, Sgambato A, Campagnolo L.** Low doses of pristine and oxidized single-wall carbon nanotubes affect mammalian embryonic development. ACS Nano 2011, **5**, 4624-4633.

22. **Riehemann K, Schneider SW, Luger TA, Godin B, Ferrari M, Fuchs H.** Nanomedicine-challenge and perspectives. Angew Chem Int Ed Engl 2009, **48**, 872-897.

23. **Semmler-Behnke M, Kreyling WG, Lipka J, Fertsch S, Wenk A, Takenaka S, Schmid G, Brandau W.** Biodistribution of 1.4- and 18-nm gold particles in rats. Small 2008, **4**, 2108-2111.

24. **Serpone N, Dondi D, Albini A.** Inorganic and organic UV filters: their role and efficacy in sunscreens and suncare products. Inorganica Chim Acta 2007, **360**, 794-802.

25. **Sun J, Wang S, Zhao D, Hun FH, Weng L, Liu H.** Cytotoxicity, permeability, and inflammation of metal oxide nanoparticles in human cardiac microvascular endothelial cells: cytotoxicity, permeability, and inflammation of metal oxide nanoparticles. Cell Biol Toxicol 2011, **27**, 333-342.

26. **Thill A, Zeyons O, Spalla O, Chauvat F, Rose J, Auffan M, Flank AM.** Cytotoxicity of CeO₂ nanoparticles for *Escherichia coli*. Physico-chemical insight of the cytotoxicity mechanism. Environ Sci Technol 2006, **40**, 6151-6156.

27. **Van Maele-Fabry G, Delhaise F, Picard JJ.** Morphogenesis and quantification of the development of post-implantation mouse embryos. Toxicol In Vitro 1990, **4**, 149-156.

28. **Wang B, Feng WY, Wang TC, Jia G, Wang M, Shi JW, Zhang F, Zhao YL, Chai ZF.** Acute toxicity of nano- and micro-scale zinc powder in healthy adult mice. Toxicol Lett 2006, **161**, 115-123.

29. **Wang Y, Aker WG, Hwang H, Yedjou CG, Yu H, Tchounwou PB.** A study of the mechanism of *in vitro* cytotoxicity of metal oxide nanoparticles using catfish primary hepatocytes and human HepG2 cells. Sci Total Environ 2011, **409**, 4753-4762.

30. **Xia T, Kovochich M, Liong M, Mädler L, Gilbert B, Shi H, Yeh JI, Zink JI, Nel AE.** Comparison of the mechanism of toxicity of zinc oxide and cerium oxide nanoparticles based on dissolution and oxidative stress properties. ACS Nano 2008, **2**, 2121-2134.

31. **Yon JM, Baek IJ, Lee SR, Kim MR, Lee BJ, Yun YW, Nam SY.** Immunohistochemical identification and quantitative analysis of cytoplasmic Cu/Zn superoxide dismutase in mouse organogenesis. J Vet Sci 2008, **9**, 233-240.

32. **Yon JM, Jung AY, Lin C, Lee JG, Jung KY, Na H, Chung MW, Lee BJ, Yun YW, Nam SY.** Teratogenic effects of nano- and micro-sized particles of zinc oxide during mouse organogenesis. J Biomed Res 2011, **12**, 103-111.

33. **Yu L, Fang T, Xiong D, Zhu W, Sima X.** Comparative toxicity of nano-ZnO and bulk ZnO suspensions to zebrafish and the effects of sedimentation, ·OH production and particle dissolution in distilled water. J Environ Monit 2011, **13**, 1975-1982.

34. **Zhu L, Chang DW, Dai L, Hong Y.** DNA damage induced by multiwalled carbon nanotubes in mouse embryonic stem cells. Nano Lett 2007, **7**, 3592-3597.

35. **Zhu X, Wang J, Zhang X, Chang Y, Chen Y.** The impact of ZnO nanoparticle aggregates on the embryonic development of zebrafish (*Danio rerio*). Nanotechnology 2009, **20**, 195103.